BULGARIAN ACADEMY OF SCIENCES

CYBERNETICS AND INFORMATION TECHNOLOGIES • Volume **24**, No 4
Sofia • 2024 Print ISSN: 1311-9702; Online ISSN: 1314-4081
DOI: 10.2478/cait-2024-0039

Transmission Map Refinement Using Laplacian Transform on Single Image Dehazing Based on Dark Channel Prior Approach

Lailia Rahmawati, Supriadi Rustad, Aris Marjuni, Mochammad Arief Soeleman, Catur Supriyanto, Guruh Fajar Shidik

Department of Informatics Engineering, Universitas Dian Nuswantoro, Semarang, Indonesia
E-mails: liaundarjombang@gmail.com srustad@dsn.dinus.ac.id aris.marjuni@dsn.dinus.ac.id arief2802@dsn.dinus.ac.id catur.supriyanto@dsn.dinus.ac.id guruh.fajar@research.dinus.ac.id

***Abstract*:** *Computer vision requires high-quality input images to facilitate image interpretation and analysis tasks. However, the image acquisition process does not always produce good-quality images. In outdoor environments, image quality is determined by weather or environmental conditions. Bad weather conditions due to pollution particles in the atmosphere such as smoke, fog, and haze can degrade image quality, such as contrast, brightness, and sharpness. This research proposes to obtain a better haze-free image from a hazy image by utilizing the Laplacian filtering and image enhancement techniques in the transmission map reconstruction based on the dark channel prior approach. Experimental results show that the proposed method could improve the visual quality of the dehazed images from 45% to 56% compared to the ground-truth images. The proposed method is also fairly competitive compared to similar methods in the same domain.*

***Keywords*:** *Dehazed image, Single image dehazing, Dark channel prior, Transmission map, Laplacian transform.*

1. Introduction

A high-quality image is one of the important components in computer vision that support the interpretation and understanding of visual information. Some applications such as safety monitoring, remote sensing, automated driving assistance, surveillance, video analysis, image classification, image segmentation, object detection, radar monitoring, and behavior analysis require quality input images [1, 3]. High-quality images can be acquired through control over some components, such as cameras, lenses, sensors, lighting, and the photographer's expertise. In the case of outdoor image acquisition, natural environmental factors such as weather and occlusion that obstruct objects also affect the quality of the acquired image [4-7]. Various adverse weather conditions caused by haze [8], fog or smoke [9, 10], rain [11], or snow [12] can obstruct visibility and blurry [13]. Particles in haze can decrease contrast and color quality caused by excessive light absorption [14].

Many researchers in computer vision have proposed many image dehazing techniques to restore a hazy image into a haze-free image so that more useful in supporting computer vision tasks such as object detection [15]. Image dehazing has become an important technique in computer vision as a pre-processing stage to improve the visual quality of hazy images [1, 2]. Image dehazing will allow computer vision analysis to progress beyond simple interpretation into more complex comprehension. Many different approaches to reducing or eliminating the haze effect in images have been suggested with different assumptions, limitations, or feature definitions. Almost all image dehazing techniques often use an atmospheric scattering model for estimating dehazed images [16].

Based on the number of reference hazy images used for the dehazing process, there are single-image dehazing and multiple-image dehazing techniques [1, 17]. Single-image dehazing uses a single hazy image to reconstruct a dehazed version, while multiple-image dehazing uses many hazy images of the same scene to reconstruct a dehazed image. Multiple image dehazing uses various polarization filters with different levels and weather conditions to restore a haze-free image from a series of hazy images. Instead of polarization filters, the other multiple image dehazing methods are suggested to use an extra segmentation [18]. Using several hazy images, several data can complement each other even though the dehazing procedure becomes more complicated, such as transmission maps and atmospheric light estimations. Some practical challenges in multiple-image dehazing [18-21] include computational complexity, input image dependency, device specification requirements, and the availability of multiple photos in the same scene in a short time [1, 19]. Because of these limitations, many researchers focus on improving single-image dehazing techniques as this technique is more realistic and efficient [22, 23].

Single-image dehazing has received much attention for recovering a hazy image. This technique requires only one hazy image and a part of additional information from a hazy image as a priori assumptions for the dehazing process [19], [23]. In recent years, some prior knowledge-based single-image dehazing methods have been suggested. T a n [26] had previously proposed a method with two presumptions that are attenuation and contrast. The hazy image has a lower contrast than the clear one. In addition, the spot attenuation is supposed to be continuous concerning distance. Although it produces a halo effect, this approach can maximize local contrast by utilizing a single hazy image [19].

Fattal proposed a single-image dehazing by considering a surface albedo and transmission map [24]. He employed independent component analysis and a Markov random field model for surface estimation. Although this approach has the potential to yield remarkable results, it is not recommended for photos with high haze density as it could render the assumption invalid [19]. K r a t z and N i s h i n o [25] suggested a factorial Markov random field, related to the Tan method [26], to estimate the scene's depth and albedo from a single hazy image. Image dehazing based on Bayesian was proposed by N i s h i n o, K r a t z and L o m b a r d i [27] for a similar purpose. Even though their approach could successfully recover dehazed images, an artifact appears in a location with a certain depth [19]. P a n d e y, G u p t a and G o e l [28] performed a histogram analysis on a foggy image that produced high and low

pixel variance. A principal component analysis is performed on three color channels in the areas with low pixel variance. Then the atmospheric light is calculated on the area with good contrast and sharpness.

Haze consists of small particles that can absorb sunlight [30]. The reflection of these particles causes a light bath or sediment. As a result, the camera when taking an image of the target object cannot produce a clear image. The distance between the camera and the target object that is obstructed by haze has a depth of distance that will affect the quality of results and image distortion [14]. Many classic approaches have been carried out by other researchers, one of which is the dual transmission method [14]. This method uses two stages in transmission map estimation. First, it takes a hazy image and its dark channels as input [31]. Then find the number of light pixels and their location from the dark channel to obtain the estimated atmosphere light in each channel. The second stage is estimating transmission using the estimated atmosphere light and reconstructing the dehazed image [32].

Many dehazing methods have been proposed to reduce or remove haze. One of the popular dehazing method approaches is the restoration method which considers the characteristics of the environment such as atmosphere light, transmission map, and also the visual quality properties such as contrast, edges, and sharpness. However, the restoration-based methods still have some issues such as color distortion, transmission map estimation errors, and edge degradation [29]. A single-image dehazing method was also proposed by H e, S u n and T a n g [33], namely the Dark Channel Prior (DCP), which is intended to overcome the shortcomings of the Tan and Fattal method [15, 22, 23]. The DCP method utilizes the principle of dark pixels in the image to estimate an atmospheric model and transmission map [1, 15, 19]. A haze-free image has at least one channel with very low intensity closest to zero. This channel is then used to estimate both atmospheric light and transmission maps [1], [15, 26-28]. The DCP method has many improvements by utilizing other filters, such as edge preservation, smoothing, bilateral, guided image, anisotropic diffusion, window adaptive, associative filters, adaptively subdivided quadtree, interpolated filters, Wiener filters, gamma correction, fuzzy theory, and fusion strategies that widely optimize transmission maps. There are also improvements to the DCP method through the use of dual transform maps [29], color attenuation prior [30], morphological reconstruction [31], and adaptive air light refinement [32].

The DCP method has advantages in terms of computational simplicity and efficiency of dehazed image reconstruction. However, this method also has disadvantages related to the loss of image sharpness due to the decrease in the main edge of the image, the presence of color shifts, or the emergence of new artifacts due to the transmission map reconstruction process due to inhomogeneous color areas [33]. Based on this background, this study is proposed to improve the DCP performance by applying the Laplacian filtering in the transmission map estimation. Laplacian filtering is proposed to deal with the edge preservation problem equipped with sharpness and brightness in the post-processing to improve the visual quality of the dehazed image. Besides, Gaussian filtering is also proposed in the pre-processing to reduce the noise of hazy input.

This paper is organized into some sections. Section 2 presents a brief theory about the DCP in image dehazing. Section 3 presents the proposed method, including the experimental design related to the proposed method. Section 4 presents the hazy image dataset that is used in this study. All image datasets in this study use outdoor images containing haze. Section 5 presents the performance measurements to evaluate the performance of the proposed method, which are peak-signal-to-noise ratio and structural similarity index measure. Section 6 presents the experimental results and discussion. Finally, Section 6 presents a conclusion of the study and findings.

2. Theoretical review

Hazy images are generally related to outdoor scenes where atmospheric conditions impact image quality. The phenomenon of haze arises due to particles such as dust, smoke, or moisture in the air, which scatter and absorb light, leading to a reduction in visibility and image clarity. The formulation of a hazy image is commonly described using the atmospheric scattering model, which provides a mathematical framework for understanding the effects of haze on images. The basic model of a hazy image is expressed as [18, 22, 25, 29]:

$$I(x) = J(x)t(x) + A(1-t(x)), \tag{1}$$

with $I(x)$ as an observed hazy image at pixel location (x), $J(x)$ being a true scene radiance, A being a global atmospheric light that usually tends to be bright or achromatic, and $t(x)$ is a transmission map that represents the fraction of light transmission [18]. The term of $J(x)t(x)$ in (1) represents a direct attenuation, where its value will decrease when the depth of the scene increases. Meanwhile, the term of $A(1-t(x))$ will increase when the depth of the scene increases.

The main task of image dehazing is to restore the image $J(x)$ from the hazy image $I(x)$ based on the estimated atmospheric light value A and the transmission map $t(x)$ [18] in (1), which is formulated as

$$J(x) = \frac{I(x)-A}{t(x)} + A. \tag{2}$$

In the DCP approach, the reconstruction of the haze-free image can be done through the dark channel image which is characterized by at least one color channel that has low intensity close to zero [18, 22, 25, 29]. This characteristic can be utilized to estimate the haze thickness and recover the scene radiance [33-35]. The dark channel image can be computed as:

$$J^{\text{dark}}(x) = \min_{y\in\Omega}\left(\min_{c\in(r,g,b)} J^{c}(y)\right), \tag{3}$$

where, J^c is the intensity for the color channel at the pixel location y with $c \in \{r, g, b\}$ of the color image channel and $\Omega(x)$ is the local patch around a pixel x. The dark channel image $J^{\text{dark}}(x)$ is selected from the minimum of the three-color channels in the $\Omega(x)$. The dark channel has three features, which are: (i) shadows, (ii) surfaces, and (iii) dark objects. The minimum value of the three-color channels can be improved by combining the atmospheric light value or adjusting the direct attenuation

value. Hence, the pixel value of the dark channel can be considered to estimate the haze density of the hazy image. The minimum intensity for the color channel [18], [29] can be determined as

$$\min_{y\in\Omega(x)} \frac{t^{c}(y)}{A^{c}} = t(x)\frac{t^{c}x)}{A^{c}} + (1-t(x)) . \tag{4}$$

The local path $\Omega(x)$ is generally constant and is estimated as a value as $t(x)$, hence the minimum value of the three-color channels [22, 25] can be written as

$$\min_{y\in\Omega(x)} \frac{I^{c}(y)}{A^{c}} = \tilde{t}(x) \min_{y\in\Omega(x)} \left(\min_{y\in\Omega(x)} \frac{J^{x}(x)}{A^{c}} \right) + (1-\tilde{t}(x)) . \tag{5}$$

Furthermore, as the $J^{\text{dark}}(x) \rightarrow 0$, t=hen the $\tilde{t}(x)$ is written as:

$$\tilde{t}(x) = 1-\omega \min_{y\in\Omega(x)} \left(\min_{c} \frac{J^{c}(y)}{A^{c}} \right), \tag{6}$$

with $\omega \in [0,1]$ is a parameter that can be utilized to maintain the depth of the image scene such that the dehazed image is close to the original haze-free image. In the case of bright images, the dark channel value becomes high and far away from zero. This will make it difficult to distinguish between hazy and haze-free areas. The DCP algorithm works on the assumption that in hazy images there will be at least some pixels in the color channel that have low intensity (dark channel). This inability makes it difficult to estimate the transmission map needed to reconstruct haze-free images. Alternative methods are needed to overcome this case, such as contrast enhancement or transmission map estimation without low intensity prior.

3. Proposed method

Based on the introduction and problem statement in Section 1, the DCP approach in image dehazing has an advantage in the simplicity and ability to produce high-quality results. However, this approach also has limitations, among them are the problems in edge preservation, color shifts, and the presence of artifacts. This paper tries to propose a DCP-based approach method, especially to overcome the three problems through the application of Laplacian filtering and image enhancement during the reconstruction process of haze-free images. In more detail, Laplacian filtering is used during transmission map reconstruction, while image enhancement is used in post-processing to improve the sharpness and brightness of the reconstructed image.

In image processing, Laplacian filtering has the advantage of enhancing image features, particularly on edges and textures. The Laplacian transform works based on the Laplacian operator, which is a second-order derivative operator that measures the rate of change of intensity values of the image. Laplacian filtering can effectively identify edges and transitions in an image. The Laplacian $L(x,y)$ of an image with pixel intensity values $I(x,y)$ is formulated as

$$L(x) - \frac{\vartheta^{2} I}{\vartheta x^{2}} + \frac{\vartheta^{2} I}{\vartheta y^{2}} . \tag{7}$$

In a two-dimensional image, the discrete Laplacian can be computed using the convolution kernel of [0 1 0; 1 –4 1; 0 1 0]. These kernels are designed to highlight areas where there is a significant change in pixel intensity. This process involves sliding the kernel over the image and computing the weighted sum of the pixel values covered by the kernel at each position. The result of applying the Laplacian filter produces an output image that emphasizes edges. Regions where pixel intensity changes sharply will have high values, while flat regions will yield low values. This characteristic makes Laplacian filtering particularly useful for edge detection.

In this proposed method, the Laplacian filtering is intended to strengthen the transmission map estimation process that preserves the edges of the dark channel image combined with the atmospheric light estimation. Technically, the proposed method introduces the modifying of the direct attenuation term. Suppose L is a Laplacian coefficient of the hazy image of size n, N is a sparse identity matrix of size n, and $\tilde{t}(x)$ is an old transmission map estimation obtained in (6). The new radiance of the dark channel is proposed by $L + \lambda N$ where is a small positive weighted parameter to strengthen the hazy image edges. The new transmission map after being filtered by Laplacian L, namely $\tilde{t}_L(\mathrm{x})$, is formulated as

$$\lambda\tilde{t}(x) = (L + \lambda N)\,\tilde{t}_L(x)\,. \tag{8}$$

The new transmission map $\tilde{t}_L(\mathrm{x})$ can be obtained by solving the linear equation of (8), that is $\tilde{t}_L(x) = (L + \lambda N)\backslash\lambda\tilde{t}(x)$. Furthermore, the edge sharpness and color brightness are further enhanced through image enhancement techniques, which are image sharpening and image brightness as post-processing steps.

The hazy input image is pre-processed by the Gaussian filter to reduce noise with the consideration that haze artifacts can be assumed as noise. In the $2D$ image processing, the Gaussian function [32] is written as

$$G(x, y; \sigma) = \frac{1}{2\pi\sigma^2} e^{-\frac{x^2+y^2}{2\sigma^2}}\,. \tag{9}$$

The Gaussian filtering is quite sensitive to noise, so it can have a significant impact on reducing haze caused by low illumination or transmission [30]. It will produce image smoothing by averaging the pixels around the area weighted by the Gaussian function. Smoothing images can reduce noise density but will also reduce the sharpness of the image edges. To address this issue, a small-sized kernel or smaller can be selected to smooth the hazy image on the low gradient without smoothing the edges. It is like a Gaussian filtering trade-off, where utilizing the value of σ is required to preserve the edges at a certain level.

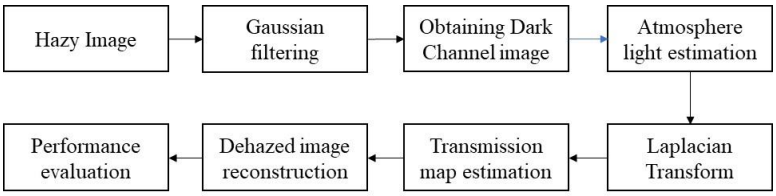

Fig. 1. Brief of the proposed method diagram

Briefly, the proposed image dehazing method based on the DCP approach has several steps comprising image preprocessing, obtaining dark channel image, atmosphere light estimation, transmission map estimation, and dehazed image reconstruction as illustrated in Fig. 1. The input of this experiment is a hazy image, while the output is dehazed image. Before the DCP approach is applied, the input hazy image is first corrected using Gaussian filtering to reduce noise in the hazy image. Next step, the dark channel image is taken from the pre-processed image to estimate an atmosphere light channel value. Furthermore, the estimated atmosphere light values are used to determine the initial transmission map. The next process improving the transmission map using the Laplace transform to obtain a new transmission map. The final step is to reconstruct the hazy-free image using the atmosphere light values and the improved transmission map. To enhance the visual quality of the dehazed image, the dehazed image reconstruction also applies image enhancement techniques, such as image sharpening and brightness.

4. Hazy image dataset

The objective of this experiment is to evaluate the performance of the DCP-based image dehazing method with a focus on the use of the Laplacian transform in the dehazed image reconstruction process.

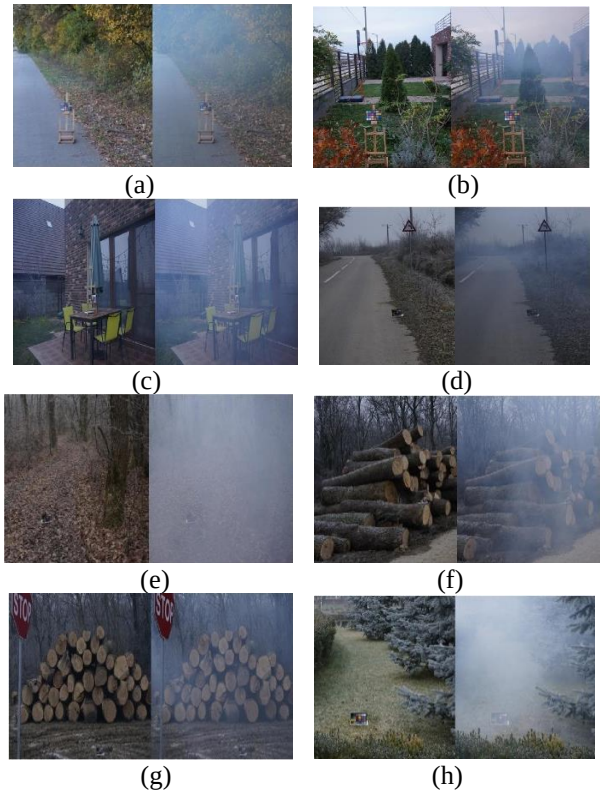

Fig. 2. Haze-free (left) and hazy images (right) of: oh1.png (a); oh2.png (b); oh3.png (c); oh4.png (d); oh5.png (e); oh6.png (f); oh7.png (g); oh8.png (h)

The experiment was conducted using the public O-HAZE dataset, which is an outdoor haze image published by A n c u t i et al. [36]. The dataset also consists of haze-free images that will be used for comparison performance analysis.

The dataset originally consisted of 45 pairs of clean and hazy images and can be downloaded at the URL: **https://data.vision.ee.ethz.ch/cvl/ntire18/o-haze/**. For analysis purposes, this experiment only uses 8 sample images of clean and hazy image pairs, namely oh1.png, oh2.png, oh3.png, oh4.png, oh5.png, oh6_hazy.png, oh7.png, and oh8.png and its hazy images as shown in Fig. 2. This dataset is color hazy images with varying levels of hazy density.

5. Performance evaluation

To evaluate the performance of the proposed method, this experiment uses two metrics, which are the Peak-Signal-to-Noise-Ratio (PSNR) and Structural Similarity Index Measure (SSIM). The PSNR is a metric used to measure the quality of a reconstructed image relative to the original image. PSNR is expressed in decibels (dB) by comparing the strength of the signal of the original image to the level of noise or errors during processing, which is computed below (see (10)). A reconstructed image with a higher PSNR value represents a low noise level of the reconstructed image and it has a better visual image quality compared to the image with lower PSNR value.

Suppose x is an original image with $M \times N$ of size and y is a reconstructed image with $M \times N$ of size, m is the maximum of the pixel value, M is the size of a row, and N is the size of a column. The PSNR [37-39, 44] between x and y is formulated by:

$$\begin{aligned} &\mathrm{PSNR}(x, y) = 10\log_{10}(\mathrm{m}^2) / \mathrm{MSE}, \\ &\mathrm{MSE} = \frac{1}{MN}\sum_{i=1}^{M}\sum_{j=1}^{N}\left(x_{(i,j)} - y_{(i,j)}\right)^2. \end{aligned} \tag{10}$$

SSIM is a metric for assessing the similarity between a reconstructed image and the original image through differences in pixel structure and visual perception aspects (luminance and contrast). Suppose x is an original image with $M \times N$ of size and y is a reconstructed image with $M \times N$ of size, the SSIM [37, 38, 40, 41, 44] between x and y is computed by:

$$\begin{aligned} &\mathrm{SSIM}(x, y) = [l(x, y)]^{\alpha}[c(x, y)]^{\beta}[s(x, y)]^{\gamma}, \\ &l(x, y) = \frac{2\mu_x\mu_y + C_1}{\mu_x^2 + \mu_y^2 + C_1}, \\ &c(x, y) = \frac{2\sigma_x\sigma_y + C_2}{\sigma_x^2 + \sigma_y^2 + C_2}, \\ &s(x, y) = \frac{2\sigma_{xy} + C_3}{\sigma_x\sigma_y + C_3}, \end{aligned} \tag{11}$$

where μ_x and μ_y are the local means of image x and y, σ_x and σ_y are the deviation standards of images x and y, σ_{xy} is a cross-covariance between x and y, and C_1, C_2, C_3 are the regularization constants for the luminance $l(x, y)$, contrast $c(x, y)$, and

structural $s(x, y)$ terms, which are formulated in (11). Similar to the PSNR value, a higher SSIM value represents a better visual quality of the reconstructed image rather than a lower SSIM. The difference between PSNR and SSIM lies in the measurement object. SSIM measures the difference between image pixel properties, namely luminance, contrast, and pixel structure, while PSNR only measures the absolute error rate or difference between pixels.

6. Results and analysis

6.1. Preprocessing

The pre-processing stage aims to improve image quality, especially for noise reduction and image smoothing using Gaussian filters. The selection of this filter considers that the Gaussian filter cannot only reduce noise and smooth an image but can also maintain image edge information to avoid losing information from the image. The PSNR values of the hazy images of oh1_hazy.png, oh2_hazy.png, oh3_hazy.png, oh4_hazy.png; oh5_hazy.png, oh6_hazy.png, oh7_hazy.png, and oh8_hazy.png are 14.68 dB, 15.61 dB, 14.99 dB, 21.76 dB, 10.95 dB, 11.62 dB, 17.35 dB, and 11.29 dB, respectively. Whereas, the PSNR values of the filtered hazy images by Gaussian filter using σ=0.5 are 14.84 dB, 15.61 dB, 15.17 dB, 22.08 dB, 11.02 dB, 11.68 dB, 17.47 dB, and 11.33 dB, respectively. All of the filtered images are presented in Fig. 5. Based on these PSNR values, the Gaussian filter provides a slight improvement in the visual quality of the images. The filtered images are presented in Fig. 3 with a standard deviation of σ=0.1.

(a) (b) (c) (d)

(d) (e) (f) (g)

Fig. 3. Filtered images by Gaussian filter with σ=0.1 of: oh1_hazy.png (a); oh2_hazy.png (b); oh3_hazy.png (c); oh4_hazy.png (d); oh5_hazy.png (e); oh6_hazy.png (f); oh7_hazy.png (g); oh8_hazy.png (h)

6.2. Obtaining dark channel images

The dark channel is the minimum value of the image of each RGB channel obtained by dividing the RGB image into local windows. The pixel value in each window is then replaced with the minimum pixel value of each channel. The dark channel transforms the hazy input image into a dark channel image of the same size as the input image with the intensity level range of [0; 1]. The dark channel images using a window size of 9×9 of oh1_hazy.png, oh2_hazy.png, oh3_hazy.png, oh4_hazy.png; oh5_hazy.png, oh6_hazy.png, oh7_hazy.png, and oh8_hazy.png are shown in Fig. 4. These dark channel images indicate that the intensity level of at least one-color channel within local windows is close to zero which represents the characteristics of an outdoor image.

The minimum intensity of the dark images of oh1_hazy.png, oh2_hazy.png, oh3_hazy.png, oh4_hazy.png; oh5_hazy.png, oh6_hazy.png, oh7_hazy.png, and oh8_hazy.png are 0.12, 0.04, 0.17, 0.09, 0.31, 0.09, 0.07, and 0.09, respectively. While the maximum intensity of the dark images of oh1_hazy.png, oh2_hazy.png, oh3_hazy.png, oh4_hazy.png; oh5_hazy.png, oh6_hazy.png, oh7_hazy.png, and oh8_hazy.png are 0.63, 0.85, 0.78, 0.53, 0.60, 0.62, 0.44 and 0.76, respectively.

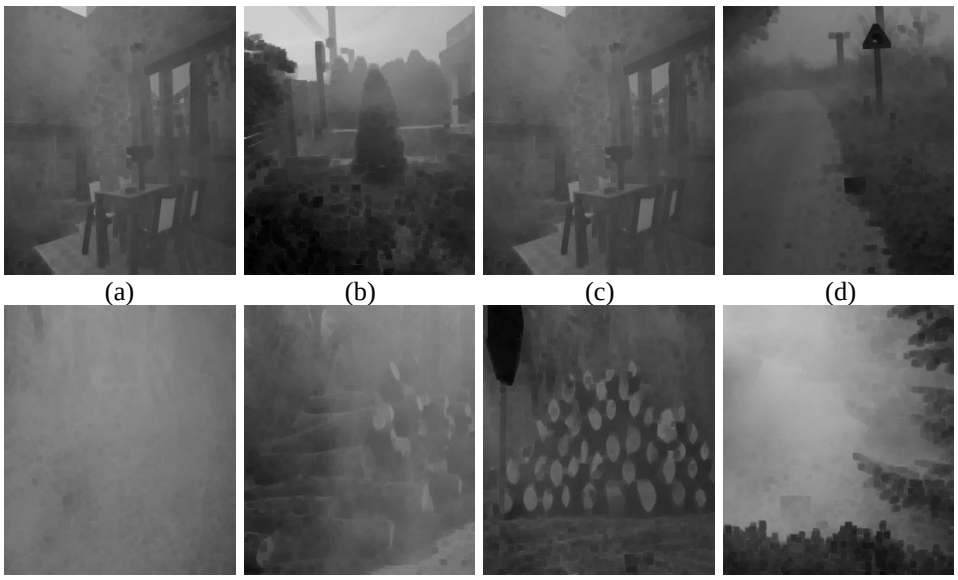

Fig. 4. Dark channel image of: oh1_hazy.png (a); oh2_hazy.png (b); oh3_hazy.png (c); oh4_hazy.png (d); oh5.png (e); oh6.png (f); oh7.png (g); oh8.png (h)

6.3. Obtaining atmosphere light channel estimation

Atmospheric light estimation is performed to estimate the light spectrum by the atmosphere that affects the image purity. The atmospheric light estimation is obtained by the dark channel by calculating the average of the percentage of the lowest pixels for each color channel. The output of this step is the estimated atmosphere light vectors containing an average of the lowest pixel values of the selected dark channel

image. Using the darkest pixels is very useful to minimize the influence of haze caused by atmospheric scattering.

The atmospheric light estimation will be used to recover the original colors of the image. The atmosphere light channel estimations of 1% of the lowest pixels of oh1_hazy.png, oh2_hazy.png, oh3_hazy.png, oh4_hazy.png; oh5_hazy.png, oh6_hazy.png, oh7_hazy.png, and oh8_hazy.png are presented in Fig. 6 on the right side, with the vector values [0.61 0.67 0.75], [0.84 0.84 0.87], [0.65 0.68 0.77], [0.53 0.56 0.62], [0.60 0.63 0.68], [0.62 0.66 0.72], [0.45 0.44 0.46], and [0.75 0.79 0.83], respectively.

6.4. Obtaining transmission map estimation

The atmosphere light values are then used to estimate the transmission map, which is computed through the dark channel and atmosphere light across the window size. The transmission map is estimated by finding the difference in color between the highest color to the weighted ratio of the dark channel and the atmosphere light values. The weight parameter value (ω) of this estimation can be set in the range of $0 \leq \omega \leq 1$. The transmission map estimation represents the estimation of the quantity of light captured by the camera after being emitted by the atmosphere. Low transmission values indicate more haze, while high transmission values indicate less haze in the hazy image. Using the weight parameter ω of 0.95 or 95%, the transmission map of oh1_hazy.png, oh2_hazy.png, oh3_hazy.png, oh4_hazy.png; oh5_hazy.png, oh6_hazy.png, oh7_hazy.png, and oh8_hazy.png are presented in Fig. 5.

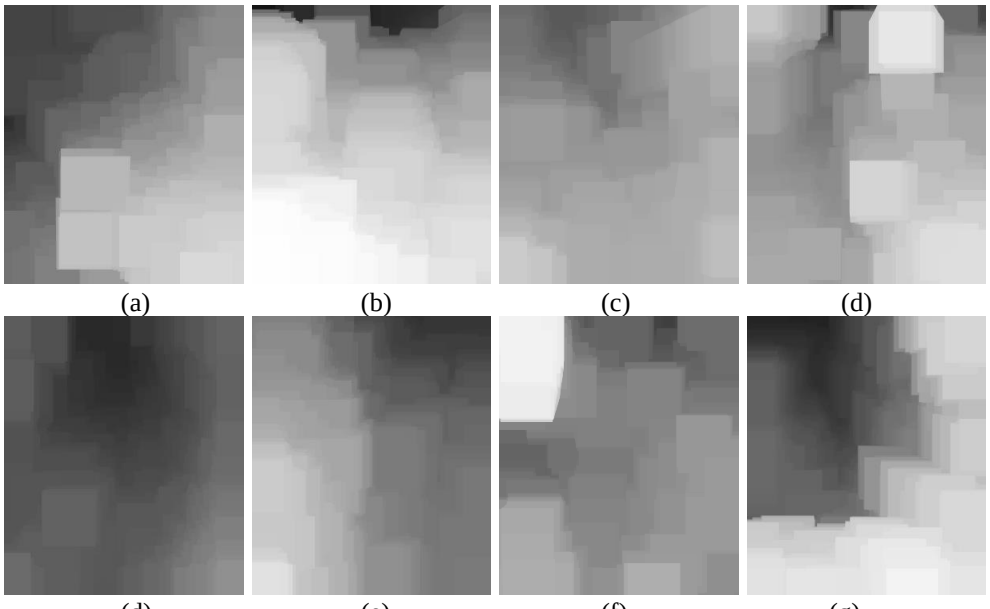

Fig. 5. Transmission map estimation of: oh1_hazy.png (a); oh2_hazy.png (b); oh3_hazy.png (c); oh4_hazy.png (d); oh5.png (e); oh6.png (f); oh7.png (g); oh8.png (h)

6.5. Dehazing using the Laplacian filter

In this experiment, the dehazed image is reconstructed by the Laplacian transform of the hazy image. The Laplacian coefficients are then used to rearrange the new transmission map with the direct attenuation weight close to zero. The use of the Laplacian coefficient is also to preserve the edge of the image, compared to the previous transmission map estimation in Fig. 5. The transmission map estimation after Laplacian filtering using λ=0.0001 is illustrated in Fig. 6.

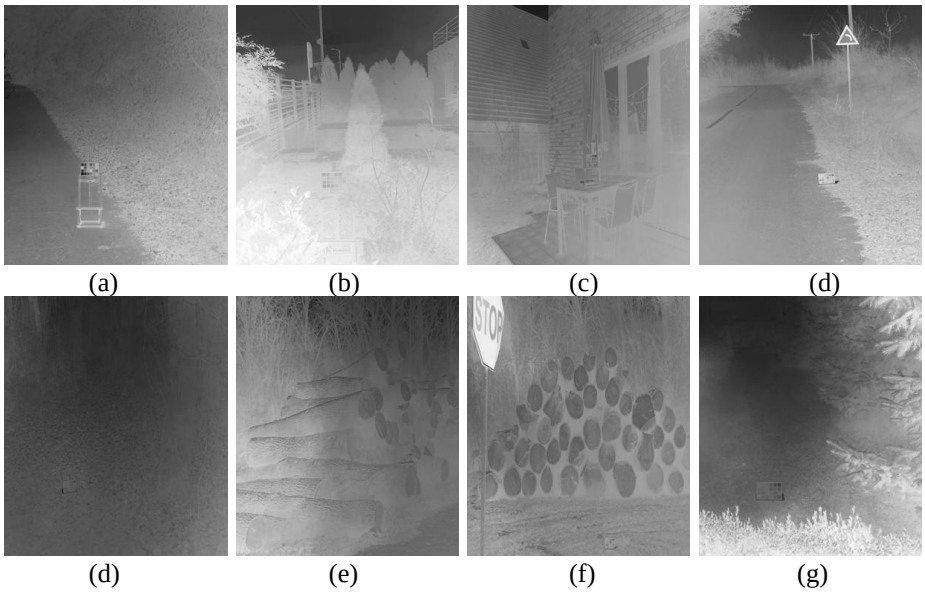

Fig. 6. Transmission map estimation after Laplacian filtering of: oh1_hazy.png (a); oh2_hazy.png (b); oh3_hazy.png (c); oh4_hazy.png (d); oh5.png (e); oh6.png (f); oh7.png (g); oh8.png (h)

The reconstruction process involves the transmission, atmosphere light, and hazy image. The reconstructed dehazed images of oh1_hazy.png, oh2_hazy.png, oh3_hazy.png, oh4_hazy.png; oh5_hazy.png, oh6_hazy.png, oh7_hazy.png, and oh8_hazy.png using an attenuation level of 0.001 are presented in Fig. 7. After reconstruction, image sharpening and brightness filtering are performed to enhance the visual quality of the dehazed image.

The PSNR and SSIM values of dehazed images of oh1_hazy.png, oh2_hazy.png, oh3_hazy.png, oh4_hazy.png; oh5_hazy.png, oh6_hazy.png, oh7_hazy.png, and oh8_hazy.png are presented in Table 1. Based on the PSNR and SSIM values, it shows that dehazed image reconstruction using Laplacian transform can increase the dehazed images for almost hazy images instead of reconstruction without Laplacian transform. It can be concluded that the use of Laplacian can contribute to the dehazed image quality through the Laplacian coefficient during reconstruction.

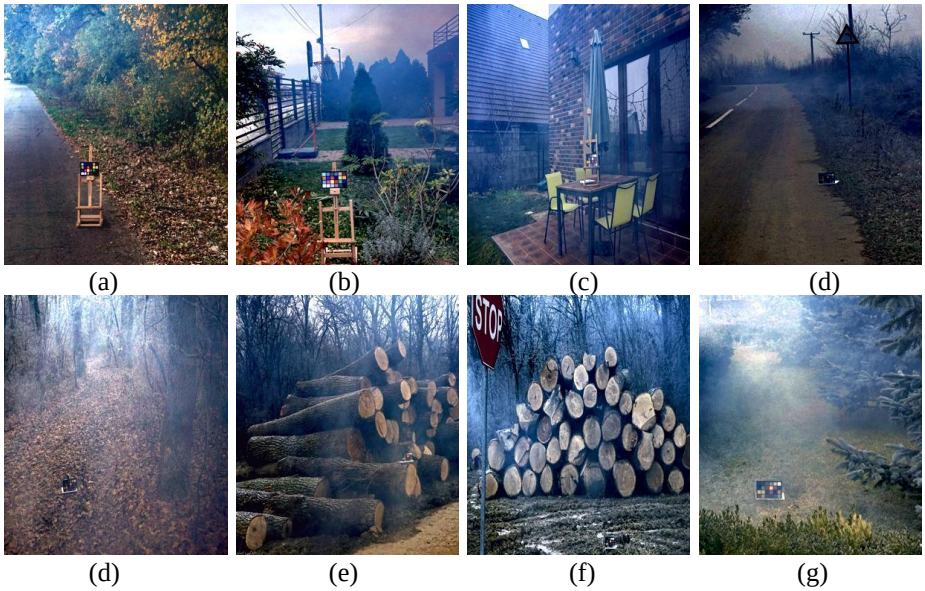

Fig. 7. Reconstructed dehazed images of: oh1_hazy.png (a); oh2_hazy.png (b); oh3_hazy.png (c); oh4_hazy.png (d); oh5_hazy.png (e); oh6_hazy.png (f); oh7_hazy.png (g); oh8_hazy.png (h)

Table 1. Performance evaluation of the proposed method

Hazy image name	PSNR (dB)			SSIM		
	Hazy image	Dehazed image without Laplacian	Dehazed image with Laplacian	Hazy image	Dehazed image without Laplacian	Dehazed image with Laplacian
oh1_hazy	14.68	13.19	13.13	0.48	0.49	0.49
oh2_hazy	15.61	15.72	16.74	0.68	0.59	0.64
oh3_hazy	14.99	16.18	16.84	0.65	0.58	0.64
oh4_hazy	21.76	15.66	16.70	0.65	0.43	0.55
oh5_hazy	10.95	12.78	12.60	0.09	0.56	0.53
oh6_hazy	11.62	15.44	15.69	0.35	0.54	0.57
oh7_hazy	17.35	13.28	13.42	0.61	0.44	0.48
oh8_hazy	11.29	12.29	13.35	0.37	0.49	0.55

6.6. Performance comparison

For evaluation of the proposed method, some DCP-based dehazing methods are used as performance comparison, such as the DCP-based dehazing proposed by Nurhayati et al. [43], Ehsan et al. [39], Zhu, Mai and Shao [40], He, Sun and Tang [33], Colores et al. [41], and Dhara et al. [42]. This comparison uses the house.png image as shown in Fig. 8, which is the ground-truth image in Fig. 8(a) and its hazy image in Fig. 8(b). The PSNR and SSIM values of the original hazy image are about 15.40 dB and 0.75, respectively.

After pre-processing using the Gaussian filter, the filtered of the house.png image is shown in Fig. 9(a), while the dark channel of the hazy image is shown in Fig. 9(b). The atmosphere light estimation value vector of the dark channel is [0.88, 0.85, 0.79]. Applying the Laplacian transform in the previous transmission map estimation produces the new transmission map image as shown in Fig. 9(c). The

reconstruction dehazed image is shown in Fig. 9(d) with the PSNR and SSIM values are 20.67 dB and 0.86, respectively. This performance achievement outperforms the performance of DCP-based image dehazing methods proposed by Nurhayati et al. [43], Ehsan et al. [39], Zhu, Mai and Shao [40], He, Sun and Tang [33], Colores et al. [41], and Dhara et al. [42], which each provide PSNR values of 16.47 dB, 14.96 dB, 11.97 dB, 14.19 dB, 9.49 dB, and 13.38 dB, respectively [42].

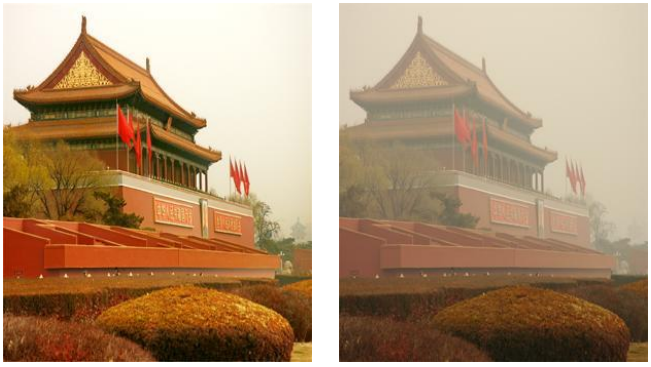

(a) (b)

Fig. 8. Ground-truth image (a), hazy image of the house.png image (b)

(a) (b) (c) (d)

Fig. 9. The house.png image of: Gaussian filtered (a); dark channel image (b); transmission map image (c); reconstructed dehazed image (d)

7. Conclusion

Transmission map reconstruction is one of the important processes in image haze removal based on the DCP approach. Normal transmission maps generally leave some issues, such as edge preservation, color shift, and artifacts. To overcome these problems, this study introduces the use of Laplacian filtering in the DCP method to reduce the haze in the image. This Laplacian filtering is intended to utilize edge preservation in the transmission map reconstruction. Mainly, the initial transmission in the DCP is enhanced by Laplacian filtering to obtain a better transmission map. That not only strengthens the transmission map but also deducts the presence of artifacts within the dehazed image. To improve the performance of the proposed method, this study uses Gaussian filtering in the pre-processing step to reduce any noise before applying the DCP. While image sharpening and brightness filtering are

used as post-processing to enhance the visual quality of the dehazed image. Although not able to remove the hazy perfectly, at least the experimental research shows that the proposed method could improve the basic image dehazing based on the DCP approach and be able to compete fairly with other similar methods.

For further work, the performance of this proposed method still needs to be improved, including finding the optimal parameter values for transmission map reconstruction, utilizing the dark channel images, and finding a better atmospheric light estimation to strengthen the transmission map reconstruction.

References

1. Harish Babu, G., N. Venkatra. A Survey on Analysis and Implementation of State-of-the-Art Haze Removal Techniques. – J. Vis. Commun. Image Represent, Vol. **72**, 2020. DOI: 10.1016/J.JVCIR.2020.102912.
2. Van Nguyen, T., A. G. Vien, C. Lee. Real-Time Image and Video Dehazing Based on Multiscale Guided Filtering. – Multimed. Tools Appl., Vol. **81**, 2022, No 25, pp. 36567-36584. DOI: 10.1007/s11042-022-13533-4.
3. Liu, Y., P. Jia, H. Zhou, A. Wang. Joint Dehazing and Denoising for Single Nighttime Image via Multi-Scale Decomposition. – Multimed. Tools Appl., Vol. **81**, 2022, No 17, pp. 23941-23962. DOI: 10.1007/s11042-022-12681-x.
4. Mirani, I. K., C. Tianhua, M. Abid, A. Khan, S. M. Aamir, W. Menhaj. Object Recognition in Different Lighting Conditions at Various Angles by Deep Learning Method. – J. Xi'an Univ. of Arch. Tech., Vol. **XIV**, 2022, No 1, pp. 158-168. DOI: 10.48550/arXiv.2210.09618.
5. Pal, N. S., S. Lal, K. Shinghal. A Robust Framework for Visibility Enhancement of Foggy Images. – Int. J. Eng. Sci. and Tech., Vol. **22**, 2019, No 1, pp. 22-32. DOI: 10.1016/j.jestch.2018.11.006.
6. Kumar, A., U. Mital, A. Gajera, S. Varanasi, A. Kumar. Empirical Study of the Impact of Image Quality, Object Size, and Occlusion on Object Detection. – EasyChair Preprint, 2023, No 9786. **https://easychair.org/publications/preprint_open/Wf1V**
7. Borel-Donohue, C. C., S. S. Young. Image Quality and Super Resolution Effects on Object Recognition Using Deep Neural Networks. – Proc. SPIE 11006, Artificial Intelligence and Machine Learning for Multi-Domain Operations Applications, 110061M, 2019. DOI: 10.1117/12.2518524.
8. Min, X., G. Zhai, K. Gu, X. Yang, X. Guan. Objective Quality Evaluation of Dehazed Images. – IEEE Transactions on Intelligent Transportation Systems, Vol. **20**, 2019, No 8, pp. 2879-2892. DOI: 10.1109/TITS.2018.2868771.
9. Ogunrinde, I., S. Bernadin. A Review of the Impacts of Defogging on Deep Learning-Based Object Detectors in Self-Driving Cars. – In: Proc. of Conf. IEEE SoutheastCon, Institute of Electrical and Electronics Engineers, Inc., 2021. DOI: 10.1109/SoutheastCon45413.2021.9401941.
10. Li, S., Q. Yuan, Y. Zhang, B. Lv, F. Wei. Image Dehazing Algorithm Based on Deep Learning Coupled Local and Global Features. – Appl. Sci. (Switzerland), Vol. **12**, 2022, No 17. DOI: 10.3390/app12178552.
11. Li, R., L. F. Cheong, R. T. Tan. Heavy Rain Image Restoration: Integrating Physics Model and Conditional Adversarial Learning. – In: Proc. of IEEE Comp. Soc. Conf. on Comp. Vision and Pattern Recogn., 2019, pp. 1633-1642. DOI: 10.1109/CVPR.2019.00173.
12. Kawarabuki, H., K. Onoguchi. Snowfall Detection in a Foggy Scene. – In: Proc. of Int. Conf. on Pattern Recogn., Institute of Electrical and Electronics Engineers, Inc., 2014, pp. 877-882. DOI: 10.1109/ICPR.2014.161.

13. M i c l e a, I. C., R. U n g u r e a n u, V. I. S a n d r u, F. D. S i l e a. Visibility Enhancement and Fog Detection: Solutions Presented in Recent Scientific Papers with Potential for Application to Mobile Systems. – Sensors, Vol. **21**, No 10, pp. 1-39. DOI: 10.3390/s21103370 Academic.
14. E h s a n, S. M., M. I m r a n, A. U l l a h, E. E l b a s i. A Single Image Dehazing Technique Using the Dual Transmission Maps Strategy and Gradient-Domain Guided Image Filtering. – IEEE Access, Vol. **9**, 2021, pp. 89055-89063. DOI: 10.1109/ACCESS.2021.3090078.
15. A l i, A. M., B. B e n j d i r a, A. K o u b a a, W. E l-S h a f a i, Z. K h a n, W. B o u l i l a. Vision Transformers in Image Restoration: A Survey. – Sensors, Vol. **23**, 2023, No 5. DOI: 10.3390/s23052385.
16. R a i k w a r, S. C., S. T a p a s w i. Lower Bound on Transmission Using Non-Linear Bounding Function in Single Image Dehazing. – IEEE Trans. on Image Proc., Vol. **29**, 2020, pp. 4832-4847. DOI: 10.1109/TIP.2020.2975909.
17. G u o, J. M., J. Y. S y u e, V. R. R a d z i c k i, H. L e e. An Efficient Fusion-Based Defogging. – IEEE Trans. on Image Proc., Vol. **26**, 2017, No 9, pp. 4217-4228. DOI: 10.1109/TIP.2017.2706526.
18. N a r a s i m h a n, S. G., S. K. N a y a r. Contrast Restoration of Weather Degraded Images. – IEEE Trans. on. Pattern Analysed and Mach. Intell., Vol. **25**, 2003, No 6, pp. 713-724. DOI:10.1109/TPAMI.2003.1201821.
19. W a n g, W., X. Y u a n. Recent Advances in Image Dehazing. – IEEE/CAA J. of Automatica Sinica, Vol. **4**, 2017, No 3, pp. 410-436. DOI: 10.1109/JAS.2017.7510532.
20. L i u, F., L. C a o, X. S h a o, P. H a n, X. B i n. Polarimetric Dehazing Utilizing Spatial Frequency Segregation of Images. – Appl. Opt., Vol. **54**, 2015, No 27, 8116. DOI: 10.1364/ao.54.008116.
21. S h w a r t z, S., E. N a m e r, Y. Y. S c h e c h n e r. Blind Haze Separation. – In: Proc. of 2006 IEEE Computer Soc. Conf. on Comp. Vision and Pattern Recogn (CVPR'06), 2006., pp. 1984-1991. DOI: 10.1109/CVPR.2006.71.
22. L e e, S., S. Y u n, J. H. N a m, C. S. W o n, S. W. J u n g. A Review on Dark Channel Prior Based Image Dehazing Algorithms. – EURASIP J. Image and Video Process., Springer International Publishing, 2016, pp. 1-23. DOI: 10.1186/s13640-016-0104-y.
23. W a n g, W., X. Y u a n, X. W u, Y. D o n g. An Airlight Estimation Method for Image Dehazing Based on Gray Projection. – Multimed. Tools Appl., Vol. **79**, 2020, No 37-38, pp. 27185-27203. DOI: 10.1007/s11042-020-09380-w.
24. F a t t a l, R. Single Image Dehazing – ACM Trans. Graph, Vol. **27**, 2008, No 3, pp. 1-9. DOI: 10.1145/1360612.1360671.
25. K r a t z, L., K. N i s h i n o. Factorizing Scene Albedo and Depth from a Single Foggy Image. – In: Proc. of 12th IEEE Int. Conf. on Comp. Vis., 2009. DOI: 10.1109/ICCV.2009.5459382.
26. T a n, R. T. Visibility in Bad Weather from a Single Image. – In: Proc. of IEEE Conf. Comp. Vis. and Pattern Recog., 2008, pp. 1-8. DOI: 10.1109/CVPR.2008.4587643.
27. N i s h i n o, K., L. K r a t z, S. L o m b a r d i. Bayesian Defogging. – Int. J. Comp. Vis., Vol. **98**, 2012, pp. 263-278. DOI: 10.1007/s11263-011-0508-1.
28. P a n d e y, P., R. G u p t a, N. G o e l. A Fast and Effective Vision Enhancement Method for Single Foggy Image. – Int. J. Eng. Sci. Tech., Vol. **24**, 2021, Issue 6, pp. 1478-1489. DOI: 10.1016/j.jestch.2021.03.014.
29. K a u r, M., D. S i n g h, V. K u m a r, K. S u n. Color Image Dehazing Using Gradient Channel Prior and Guided L0 Filter. – Inf. Sci., Vol. **521**, 2020, pp. 326-342. DOI: 10.1016/j.ins.2020.02.048.
30. T r i v e d i, V. K., P. K. S h u k l a, H. G u p t a. Dark Channel Prior and Global Contrast Stretching Based Hybrid Defogging Image Technique. – In: Proc. of 2018 Int. Conf. on Adv. Comp. and Telec., 2018. DOI: 10.1109/ICACAT.2018.8933729.
31. L i, Z, J. Z h e n g. Single Image De-Hazing Using Globally Guided Image Filtering. – IEEE Trans. Image Proc., Vol. **27**, 2018, No 1, pp. 442-450. DOI: 10.1109/TIP.2017.2750418.
32. K o k u l, T., S. A n p a r a s y. Single Image Defogging Using Depth Estimation and Scene-Specific Dark Channel Prior. – In: Proc. of 20th Int. Conf. on Adv. in ICT for Emerging Reg., Institute of Electrical and Electronics Engineers Inc., 2020, pp. 190-195. DOI: 10.1109/ICTer51097.2020.9325450.

33. He, K., J. Sun, X. Tang. Single Image Haze Removal Using Dark Channel Prior. – IEEE Trans Pattern Anal. Mach. Intell., Vol. **33**, 2011, No 12, pp. 2341-2353. DOI: 10.1109/TPAMI.2010.168.
34. Iwamoto, Y., N. Hashimoto, Y. W. Chen. Real-Time Haze Removal Using Normalised Pixel-Wise Dark-Channel Prior and Robust Atmospheric-Light Estimation. – Appl. Sci., Vol. **10**, 2020, No 1165, pp. 1-13. DOI: 10.3390/app10031165.
35. Musunuri, Y. R., O. S. Kwon. Haze Removal Based on Refined Transmission Map for Aerial Image Matching. – Appl. Sci., Vol. **11**, 2021, No 15. DOI: 10.3390/app11156917.
36. Ancuti, C. O., C. Ancuti, R. Timofte, C. D. Vleeschouwer. O-HAZE: A Dehazing Benchmark with Real Hazy and Haze-Free Outdoor Images. – In: Proc. of IEEE Comp. Soc. Conf. on Comp. Vis. and Pattern Recog. Workshops, 2018, pp. 867-875, 2018. DOI: 10.1109/CVPRW.2018.00119.
37. Peng, Y. T., Z. Lu, F. C. Cheng, Y. Zheng, S. C. Huang. Image Haze Removal Using Airlight White Correction, Local Light Filter, and Aerial Perspective Prior. – IEEE Trans. Circuits and Sys. Video Tech., Vol. **30**, 2020, No 5, pp. 1385-1395. DOI: 10.1109/TCSVT.2019.2902795.
38. Ngo, D., G. D. Lee, B. Kang. Improved Color Attenuation Prior for Single-Image Haze Removal – Appl. Sci., Vol. **9**, 2019, No 19, pp. 1-22. DOI: 10.3390/app9194011.
39. Ehsan, S. M., M. Imran, A. Ullah, E. Elbasi. A Single Image Dehazing Technique Using the Dual Transmission Maps Strategy and Gradient-Domain Guided Image Filtering. – IEEE Access, Vol. **9**, 2021, pp. 89055-89063. DOI: 10.1109/ACCESS.2021.3090078.
40. Zhu, Q., J. Mai, L. Shao. A Fast Single Image Haze Removal Algorithm Using Color Attenuation Prior. – IEEE Trans. Image Process., Vol. **24**, 2015, No 11, pp. 3522-3533. DOI: 10.1109/TIP.2015.2446191.
41. Colores, S. S., E. C. Yepez, J. M. R. Arreguin, G. Botella, L. M. L. Carrillo, S. Ledesma. A Fast Image Dehazing Algorithm Using Morphological Reconstruction. – IEEE Trans. Image Process., Vol. **28**, 2019, No 5, pp. 2357-2366. DOI:10.1109/TIP.2018.2885490.
42. Dhara, S. K., M. Roy, D. Sen, P. K. Biswas. Color Cast Dependent Image Dehazing via Adaptive Airlight Refinement and Nonlinear Color Balancing. – IEEE Trans. Circ. Syst. Video Tech., Vol. **31**, 2021, No 5, pp. 2076-2081. DOI: 10.1109/TCSVT.2020.3007850.
43. Nurhayati, O. D., B. Surarso, W. A. Syafei, D. M. K. Nugraheni. Gaussian Filter-Based Dark Channel Prior for Image Enhancement. – Int. J. Elect. Comp. Eng., Vol. **14**, 2024, No 5, pp. 5765-5778. DOI: 10.11591/ijece.v14i5.pp5765-5778.
44. Marjuni, A., A. Z. Fanani, O. D. Nurhayati. Visual Quality Improvement of Watermarked Image Based on Singular Value Decomposition Using Walsh Hadamard Transform. – Cybernetics and Information Technologies, Vol. **23**, 2023, No 1, pp. 110-124.

Received: 14.10.2024. Second version: 07.11.2024. Third version: 13.11.2024;
Accepted: 15.11.2024. Fast-track.